Provided for non-commercial research and education use.
Not for reproduction, distribution or commercial use.

This article appeared in a journal published by Elsevier. The attached copy is furnished to the author for internal non-commercial research and education use, including for instruction at the authors institution and sharing with colleagues.

Other uses, including reproduction and distribution, or selling or licensing copies, or posting to personal, institutional or third party websites are prohibited.

In most cases authors are permitted to post their version of the article (e.g. in Word or Tex form) to their personal website or institutional repository. Authors requiring further information regarding Elsevier's archiving and manuscript policies are encouraged to visit:

http://www.elsevier.com/copyright

Author's personal copy

Materials Science in Semiconductor Processing 13 (2010) 162–166

Contents lists available at ScienceDirect

Materials Science in Semiconductor Processing

journal homepage: www.elsevier.com/locate/mssp

Influence of N_2- and Ar-ambient annealing on the physical properties of SnO_2:Co transparent conducting films

A. Gholizadeh [a,b,*], N. Tajabor [a]

[a] Department of Physics, Ferdowsi University of Mashhad, Mashhad, P.O. Box 91775-1436, Iran
[b] School of physics, Damghan university, Damghan, Iran

ARTICLE INFO

Available online 19 November 2010

Keywords:
Transparent conducting oxide
Dilute magnetic semiconductors
Spray pyrolysis

ABSTRACT

Co-doped SnO_2 TCOs were prepared by spray pyrolysis technique and the influence of N_2- and Ar-ambient annealing on their structural, electrical and optical properties was studied. XRD results show that all samples become single phase after post-annealing treatments. In addition, the Co-doped films exhibit a faceting characteristic that is conserved after the post-annealing treatments. Analysis of the XRD patterns shows that the size of crystallite decreases with increasing microstrain and both of them reach extremum at about 20 at% doping level. Electrical measurements demonstrate gradual increase in resistivity with increasing doping level. The annealing causes increase in the electrical resistivity of the cobalt-doped samples. About 40% of this increase should be due to penetration of nitrogen ions within the rutile structure and the remaining 60% may be attributed to the structural and compositional relaxations. The optical spectra show that transparency of the samples in the visible region decreases between 10% and 40% with increasing cobalt content. Although transparency of the samples at lower than 30 at% doping level slightly increases after post-annealing treatments, this increase is compensated for by compositional relaxations in the samples with more cobalt content. The band gap energies are increased by about 1.5% by post annealing treatment.

© 2010 Elsevier Ltd. All rights reserved.

1. Introduction

SnO_2 is a wide-band-gap semiconductor with bandwidth E_g=3.6–4.2 eV. In addition to excellent optical transparency, it is very stable chemically [1–13]. It is known that electrical resistivity of thin films of SnO_2 depends on concentration of oxygen vacancies within their rutile crystal structure (S.G. P4/nmm) [14]. During the last decade, large attention has been paid to tuning of oxygen vacancies by doping various metallic elements, changing the deposition technique and annealing at certain atmospheres [15–19]. Previous results show that substitution of a few percent of Sn^{4+} ions by Co^{2+} affects concentrations of oxygen vacancies and charge carriers. Ogale et al. [12] prepared Co-doped SnO_2 films by pulsed laser technique, which leads to room temperature ferromagnetism with a Curie temperature (T_C) as high as 650 K. Remarkably, at low doping concentration, a giant magnetic moment of $7.5 \pm 0.5\ \mu_B$/Co was also observed, which has not been seen in any DMS system thus far [20,21]. Hence SnO_2:Co films are potentially interesting DMSs for application in new spintronic and magneto-optic devices.

In this work, Co-doped SnO_2 films with various doping levels have been deposited using the spray pyrolysis technique. Then the structural, electrical and optical properties of the prepared samples have been studied. In the study of SnO_2 crystallites, (1 1 0), (1 0 1) and (1 0 0) are recognized as three significant crystallographic planes. Previous theoretical and experimental results indicate that (1 1 0) plane has the lowest surface energy and thus stability [22]. Surface energy, which is the characteristic parameter of the faceting behavior of SnO_2 polycrystals, depends on the chemical potential of oxygen and its deviation from surface stoichiometry. Considering that

* Corresponding author. Tel.: +98 511 8793912; fax: +98 511 8796416.
E-mail addresses: ah_gh1359@yahoo.com (A. Gholizadeh), ntajabor@yahoo.com (N. Tajabor).

1369-8001/$ - see front matter © 2010 Elsevier Ltd. All rights reserved.
doi:10.1016/j.mssp.2010.10.004

Author's personal copy

the chemical stoichiometry of planes is affected by the deposition method and post-annealing of the deposited films at certain atmospheres, we expect that the faceting behavior of the Co-doped SnO_2 samples may be controlled by changing these parameters. Therefore, the effects of N_2- and Ar-ambient annealing on the faceting, electrical and optical properties of Co-doped SnO_2 films are studied.

2. Experimental

2.1. Material preparation and deposition of films

The undoped SnO_2 thin films were deposited using an aqueous ethanol solution including $SnCl_2 \cdot 2\,H_2O$, H_2O and CH_3CH_2OH with the same weight percentage (1:1:1) and a few ml of hydrochloric acid by the spray pyrolysis technique. Also, Co-doped SnO_2 films have been prepared using 0, 2, 4, 8, 10, 12 and 14 wt% of $CoCl_2 \cdot 6H_2O$, which were added to the initial solution without any changes in the clarity of the solution. The spray solution compositions and atomic concentration ratios in the prepared solutions are given in Table 1.

Firstly, for deposition of films, glass substrates (commercial glass substrates with 1 mm thickness and $25 \times 75\ mm^2$ dimensions) were cleaned and placed on a hot plate. The hot plate temperature was kept in the range $480-500\ ^\circ C$, which is known to be optimal for the formation of SnO_2 films. After reaching 500 °C, the solution was sprayed on the hot glass substrates under the following conditions: carrier-gas-pressure (O_2), 1.7–2 atm; flow rate of solution 14 ml/min;, solution volume, $10\ cm^3$ and substrate–nozzle distance, 45 cm. All samples were prepared at almost the same conditions. The metallic salt solution, when sprayed onto a hot substrate pyrolitically it decomposes, and a chemical reaction takes place on the heated substrate and at least a thin layer of SnO_2 (undoped or doped) is deposited. Thin films of about 0.4 μm thickness are prepared in this manner as estimated by SEM micrographs and optical method. After deposition, the original thin samples were cut into $13 \times 26\ mm^2$ dimensions and four similar series of the Co-doped SnO_2 films were prepared for executing post-annealing treatments. Below, we will refer to each one of these series in the following manner. SnO_2:Co transparent conducting films prepared with different Co concentrations: (**Series 1**) as-deposited, (**Series 2)** annealed in a quartz tube furnace at 550 °C in Ar for 5 h, (**Series 3**) annealed at 550 °C in N_2 atmospheres for 5 h and (**Series 4)** annealed at 550 °C in Ar for 5 h followed by N_2 for 5 h.

Table 1
Composition of the Co-doped SnO_2 solutions.

$CoCl_2 \cdot 6H_2O$ (wt% in solution)	$SnCl_2 \cdot 2H_2O$ (M)	$CoCl_2 \cdot 6H_2O$ (M)	[Co]/[Sn] (at% in solution)
0	14.6	0	0
2	14.6	0.73	5
4	14.6	1.46	10
8	14.6	2.92	20
10	14.6	3.65	25
12	14.6	4.30	30
14	14.6	5.11	35

2.2. Structural

Step scanned powder X-ray diffraction (XRD) of undoped and Co-doped SnO_2 films were performed at room temperature in a D8 Advance Bruker system using Cu K_α (λ=0.154056 nm) radiation. Phase analysis of the samples was performed based on the XRD patterns. The information on microstrain (ε_s) and crystallite size (D) of the deposited films have been obtained from the full width at half maximum (FWHM) of the diffraction peaks (β) via the Williamson–Hall relation [23]

$$\frac{\beta\cos\theta}{\lambda} = \frac{1}{D} + \frac{\varepsilon_s \sin\theta}{\lambda} \quad (1)$$

Lattice parameter refinements were performed using CELREF software from LMGP Institute (Grenoble, France).

2.3. Electrical

Electrical measurements consisting of resistivity, carrier concentration and mobility determination were conducted via the Van der Pauw method [24]. In addition, Seebeck's effect measurements were performed for identification of the carrier type.

2.4. Optical

Absorption coefficient is a suitable quantity for studying band gap energy. Optical transmission and absorption spectra of the Co-doped SnO_2 films between 200 and 1000 nm wave lengths have been recorded at room temperature using a HP-UV–vis system (Agilent 8453, model). For estimating band gap, the optical absorption coefficient ($\alpha(\lambda)$) was calculated from the absorption spectra ($A(\lambda)$) using the following equation:

$$\alpha(\lambda) = 2.303\frac{A(\lambda)}{t} \quad (2)$$

where t is the thickness of the deposited film. Considering that the following relation holds between the optical absorption coefficient, $\alpha(\lambda)$, and the optical band gap energy of a direct band gap semiconductor [25]

$$(\alpha h\nu) = B(h\nu - E_g)^{1/2} \quad (3)$$

where B is an energy-independent constant, Band gap energy of the samples is estimated by extrapolating the linear part of $(\alpha h\nu)^2$ vs. $h\nu$ plots.

3. Results and discussion

The XRD patterns of the samples are shown in Fig. 1. It is clear that the as-deposited samples are finely polycrystalline and some of the Co-doped films are predominantly oriented. This preferential orientation and faceting behaviors can be observed in Fig. 2, where the normalized intensities of the (1 1 0), (1 0 1), (2 0 0) and (2 1 1) Brag peaks are plotted as a function of cobalt content for the series 1 samples. Comparative analysis of the XRD patterns indicates that the faceting characteristics are conserved after post annealing treatments. It is clear that the ratio of the intensity of (2 0 0) diffraction peaks considerably increases with concentration of Co impurities increasing to 25 at%. Analyses of these results

Author's personal copy

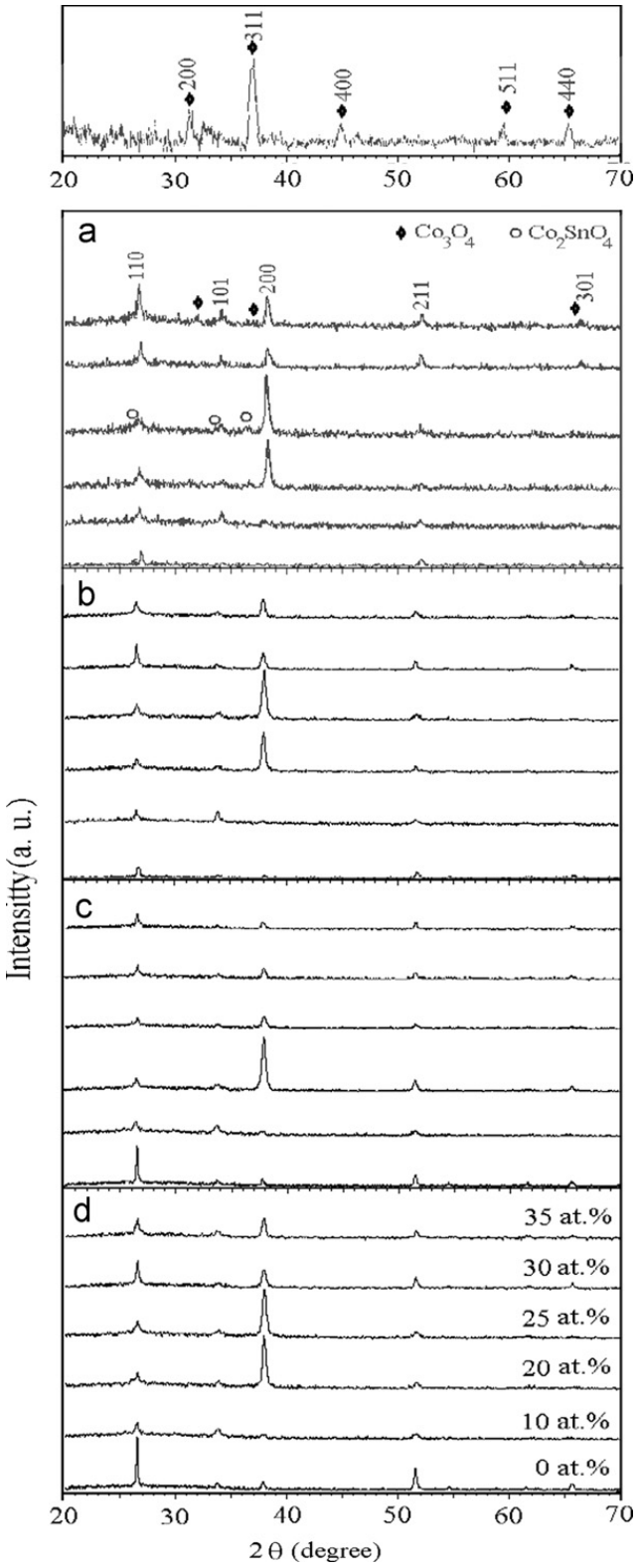

Fig. 1. XRD patterns of SnO_2:Co transparent conducting films prepared with different Co concentrations: (a) as-deposited, (b) annealed at 550 °C in Ar for 5 h, (c) annealed at 550 °C in N_2 atmospheres for 5 h and (d) annealed at 550 °C in Ar followed by N_2 for 5 h. The XRD pattern of Co_3O_4 is also given on the top of figure.

show the faceting of films along tetragonal *a*-axis, especially for the samples with 20 and 25 at% impurity levels. The preferential alignment usually originates from the strains created during deposition of films,

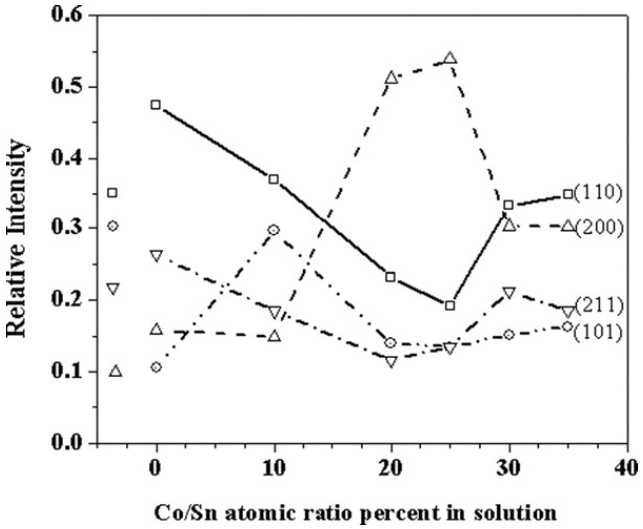

Fig. 2. Normalized intensity of the (1 1 0), (1 0 1), (2 0 0) and (2 1 1) Brag peaks of series 1 samples vs. Co/Sn atomic ratio. Normalized intensities were deduced by dividing the intensity of each peak by the sum of intensities of all the 4 peaks. Also, normalized intensities in the standard pattern of SnO_2 powder have been represented on the left hand side of the figure by appropriate symbols.

which are a function of deposition parameters such as substrate temperature and deposition rate [15]. Here, the observed faceting can be attributed to the decrease in surface energy density of the (2 0 0) plane with respect to that of (1 1 0) after partial substitution of Sn by Co [22]. Comparison of the sharpnesses of diffraction peaks of the undoped films indicates that intensity of (1 1 0) peak considerably increases with annealing in N_2 ambient but intensity of the (2 0 0) peak of the Co-doped films decreases, while Ar ambient has no such effect. This indicates that the Co-doped films become poor in crystallinity by N_2-ambient annealing.

There is no appreciable peaks shift in films beyond the 20 at% doping level. This suggested that most Co atoms are not in the SnO_2 lattice beyond the 20 at% doping level. As shown in Fig. 1, some additional peaks appear in the XRD pattern in the series 1 sample with more than 20 at% doping level. These additional peaks correspond to the standard diffraction pattern of Co_2SnO_4 and Co_3O_4 phases with cubic structures. The presence of such phases is also reported in $Zn_{1-x}Co_xO$ [26] and $Sn_{1-x}Co_xO_2$ [27] samples, which may affect the structural, electrical and optical properties of the studied samples. The unwanted phases considerably decrease after annealing and all the annealed samples seem to be of single phase.

The derived rutile lattice parameters of the series 1 sample are given in Fig. 3. This figure shows that the '*a*' and '*V*' parameters of the tetragonal unit cell decrease with increasing cobalt content, while the '*c*' parameter passes through a minimum for 20 at% doping level. The calculated lattice parameters of the annealed samples exhibit similar behavior as well. It is well known that the ionic radius of Co^{3+} (0.63 Å) is small, while the ionic radius of Co^{2+} (0.72 Å) is greater than that of Sn^{4+} (0.71 Å) [28]. Therefore, decreases in *a* and *V* are a natural consequence of the substitution of Co^{3+} ions instead of Sn^{4+} in the SnO_2 rutile structure. In addition, Fig. 1 shows a shift of peaks towards the lower diffraction angle in films after annealing in N_2 and Ar, which may be due to the chemisorptions of N_2 on the surfaces of films after annealing in N_2. Ogale et. al. [12] reported such a shift in Co-doped SnO_2 films after annealing in Ar.

In addition, the observed increase in full width at half maximum (FWHM) of the XRD peaks with increasing Co content indicates possible changes in the crystallite size and microstrains. The crystallite sizes and microstrains have been calculated based on the (1 1 0), (2 0 0) and (1 0 1) Brag peaks in the XRD patterns (Fig. 4). These results show that the size of the crystallite decreases with increasing microstrain (and conversely), and both of them reach extremum at about 20 at% doping level. In fact, a minimum of the *c* parameter is accompanied by the minimum size of crystallites and the maximum value of microstrains. So, one may attribute the abnormal minimum in the *c* lattice parameter to increase in introduced stress after substitution of Sn by Co in the rutile structure. Also, decrease in the microstrains below 20 at% doping level is compensated for by the formation of Co_2SnO_4 and Co_3O_4 unwanted phases in the

Author's personal copy

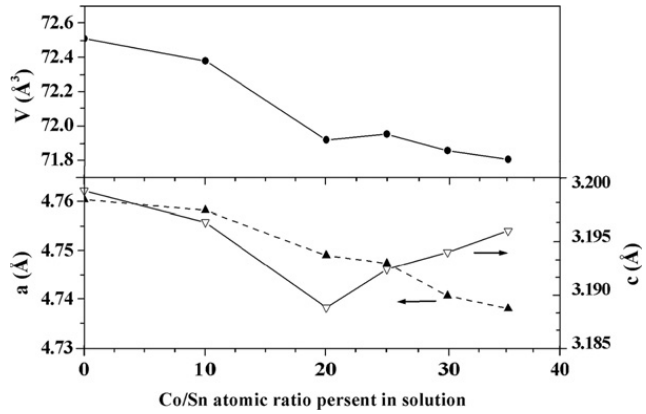

Fig. 3. Variation in crystal lattice parameters of series 1 samples vs. Co/Sn atomic ratio.

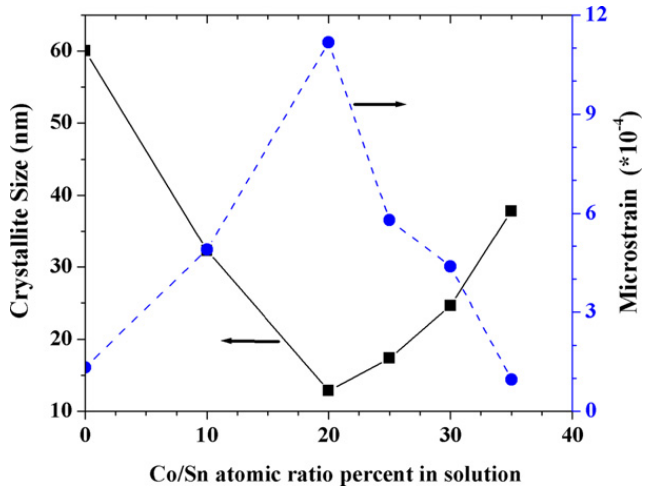

Fig. 4. Crystallite sizes and microstrains calculated based on the (1 1 0), (2 0 0) and (1 0 1) Brag peaks in the XRD patterns of series 1 samples vs. Co/Sn atomic ratio.

Table 2
Resistivity (ρ), carrier concentration (n) and Seebeck's coefficient (α) of the series 1 samples.

Sample (at%)	Thickness (nm)	ρ (Ω cm)	n × 10^{16} (cm^{-3})	α (μV/K)
0	~400	0.025	−766.00	−140
5	~400	2.32	−1.27	−75
10	~400	4.23	−0.77	−60
20	~400	5.12	−0.59	−50
25	~400	16.50	−0.69	−50
30	~400	25.00	−0.67	−55
35	~400	28.10	−0.64	−65

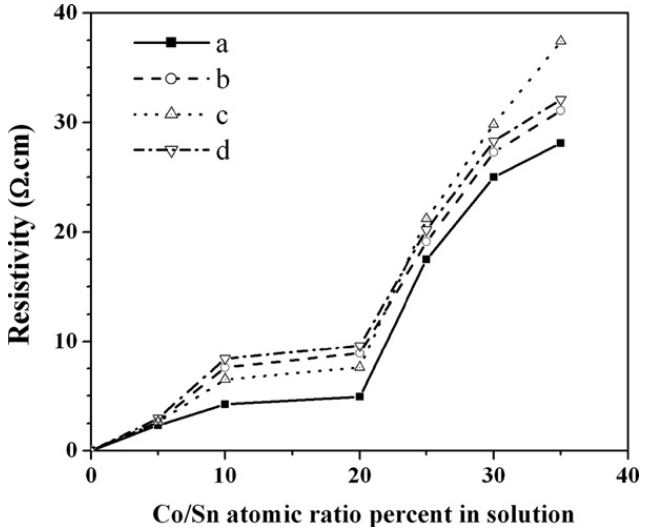

Fig. 5. Electrical resistivity of SnO_2:Co transparent conducting films prepared with different Co concentrations: (a) as-deposited, (b) annealed at 550 °C in Ar, (c) in N_2 atmospheres for 5 h and (d) in Ar followed by N_2 for 5 h.

series 1 samples. Comparison of the sharpnesses of diffraction peaks of the undoped films indicate that the size of crystallites considerably increases with annealing in N_2 ambient, while Ar ambient has no such effect. The crystal sizes were nearly the same in Co-doped films before and after annealing in N_2 and Ar.

Results of the electrical measurements exhibit a gradual increase in resistivity with cobalt additives for series 1 (Table 2). Also, the carrier concentration decreases with increasing Co content to 20 at%, and then remains approximately constant with additional doping level. The decrease in n-type carrier concentration can be attributed to the substitution of Sn^{4+} by smaller Co^{3+} in the rutile unit cell. Although by this trend, one may expect the type of carriers to gradually change from n− to p+ with increase in doping level, the results of the Seebeck's measurements emphasize the presence of n-type carriers in all studied samples. This can be explained considering that the XRD patterns show the complete penetration of Co atoms within crystal structure of SnO_2 only for lower than 20 at% doping levels. Therefore, increase in resistivity, only for lower than 20 at% doping levels, can be explained as due to decreasing carrier concentration. Increase in resistivity beyond 20 at% Co could be due to additional impurity phases, e.g. Co_3O_4 and Co_2SnO_4.

Results of electrical measurements after annealing are shown in Fig. 5. Resistivity of the undoped film decreases with annealing in N_2. When the SnO_2 film is annealed in N_2, N_2 gas is likely to react with the top oxygen layer of the film to produce NO_x and create oxygen vacancies [29]. Also, it is clear that the N_2- and Ar-ambient annealings cause increase in electrical resistivity of the cobalt-doped samples and this increase is mostly a function of the annealing duration. In addition, comparison of the effects of N_2- and Ar-ambient annealings on resistivity indicates that about 40% of this increase is due to penetration of the nitrogen ions within the rutile structure. Structural and compositional relaxations should be origins of the remaining 60% of the increase in resistivity. Increase in the resistivity of Co-doped SnO_2 films is also reported in Co-doped SnO_2 [12] films in Ar-ambient annealing. Resistivity ρ is proportional to the reciprocal of the product of carrier concentration n and mobility μ. Nitrogen was chemisorbed readily as an acceptor on the Co-doped SnO_2 surface and into the pores of the films, which decreased the electron concentration in the films due to poor crystallinity of Co-doped films by N_2-ambient annealing. Variation in mobility in terms of carrier concentration is due to a combination of ionized impurity and grain boundary scattering mechanisms, where the former seems to be dominated [30,31].

The optical transmittance of the samples at the typical 600 nm wavelength is shown in Fig. 6. These results show that transparency in the visible region decreases between 10% and 40% by increasing cobalt content. Otherwise, transparency of the samples with lower than 10 wt% doping level is slightly increased after post annealing treatments. However, this increase is compensated for by compositional relaxations in the samples with more cobalt content. The observed increase may be ascribed to the decrease in surface defects due to post annealing treatments [32].

The derived band gap energies are shown in Fig. 7, which in all samples become minimized at about 10 at% doping level. This behavior is comparable to that found in thin films with minimum band gap [26]. However, these energies are increased somewhat in the films with post-annealing treatment, which may be attributed to defect concentration and crystalline perfection.

Author's personal copy

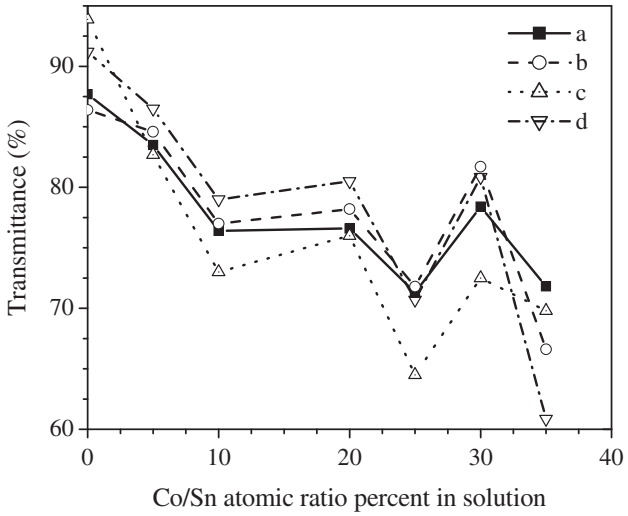

Fig. 6. Optical transmittance of SnO_2:Co transparent conducting films prepared with different Co concentrations: (a) as-deposited, (b) annealed at 550 °C in Ar, (c) in N_2 atmospheres for 5 h and (d) in Ar followed by N_2 for 5 h.

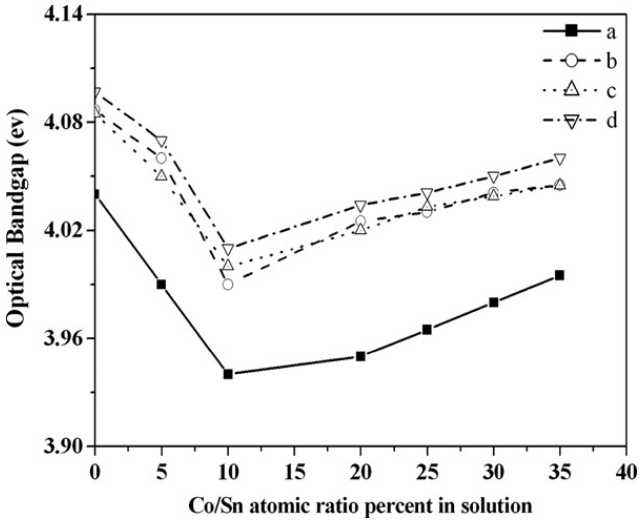

Fig. 7. Variations in the band gap energy of SnO_2:Co transparent conducting films prepared with different Co concentrations: (a) as-deposited, (b) annealed at 550 °C in Ar, (c) in N_2 atmospheres for 5 h and (d) in Ar followed by N_2 for 5 h.

4. Summary

Co-doped SnO_2 TCOs were prepared by spray pyrolysis technique and the influence of N_2- and Ar-ambient annealing on their structural, electrical and optical properties was studied. XRD patterns show that some of the Co-doped films exhibit a faceting characteristic that is conserved after post-annealing treatments. This faceting is attributed to the decrease in the surface energy density of the (2 0 0) plane with respect to that of (1 1 0) after substitution of Sn by Co. Analysis of the XRD patterns show that the size of crystallite decreases with increase in microstrain and both of them reach extremum at about 20 at% doping level. In addition, *a* and *V* parameters of the tetragonal unit cell decrease with increasing impurity content, while *c* parameter passes through a minimum at 20 at% impurity level. Electrical measurements demonstrate gradual increase in the resistivity with increasing doping level. Annealing causes increase in the electrical resistivity of the cobalt-doped samples and this increase is mostly a function of the annealing duration. About 40% of this increase should be due to penetration of the nitrogen ions within the rutile structure and the remaining 60% may be attributed to the structural and compositional relaxations. The optical spectra show that the transparency of the samples in the visible region decreases between 10% and 40% with increasing cobalt content. However, transparency of the samples with lower than 30 at% doping level slightly increases after post annealing treatments. The band gap energies are minimized at about 10 at% doping level, while these are increased somewhat with post-annealing treatment. The observed band gap variations may be attributed to defect concentration and crystalline perfection.

References

[1] Lewis BG, Paine DC. MRS Bulletin 2000:22–7.
[2] Gordon RG. MRS Bulletin 2000:52–7.
[3] Dietl T. Nature Materials 2003;2:646.
[4] Prellier W, Fouchet A, Mercey B. Journal of Physics: Condensed Matter 2003;15:R1583 Refs. 54, 55 therein.
[5] Matsukura F, Ohno H, Dietl T. III–V ferromagnetic semiconductors. In: Busschow KHJ, editor. Handbook of magnetic materials, vol. 14. Elsevier Science; 2002 [Chapter 1].
[6] Ohno H. Science 1998;281:951.
[7] Matsumoto Y, Murakami M, Shono T, Hasegawa T, Fukumura T, Kawasaki H, Ahmet P, Chikyow T, Koshihara S-Y, Koinuma H. Science 2001;291:854.
[8] Costa-Kramer JL, Briones F, Fernandez JF, Caballero AC, Villegas M, Diaz M, Garcia MA, Hernando A. Nanotechnology 2005;16:214.
[9] Kundaliya DC, Ogale SB, Lofland SE, Dahr S, Metting CJ, Shinde SR, Ma Z, Varughese B, Ramanujachary KV, Salamanca-Riba L, Venkatesan T. Nature Materials 2004;3:709.
[10] Budhani RC, Pant P, Rakshit RK, Senapati K, Mandal S, Pandey NK, Kumar J. Journal of Physics: Condensed Matter 2005;17:75.
[11] Saeki H, Matsui H, Kawai T, Tabata H. Journal of Physics: Condensed Matter 2004;16:S5533.
[12] Ogale SB, et al. Physical Review Letters 2003;91:1–4.
[13] Ji Z, He Z, Song Y, Liu K, Xiang Y. Thin Solid Films 2004;460:324–6.
[14] Batzill M, Burst JM, Diebold U. Thin Solid Films 2005;484:132–9.
[15] Korotcenkov G, Cornet A, Rossinyol E, Arbiol J, Brinzari V, Blinov Y. Thin Solid Films 2005;471:310–9.
[16] Batzill M, Diebold U. Progress in Surface Science 2005;79:47–154.
[17] Patil PS. Materials Chemistry and Physics 1999;59:185–98.
[18] Korotcenkov G, Macsanov V, Brinzari V, Tolstoy V, Schwank J, Cornet A, Morante J. Thin Solid Films 2004;467:209–14.
[19] Huang CJ, Shih WC. Journal of Electronic Materials 2003;32(10).
[20] Bagheri-Mohagheghi MM, Shokooh-Saremi M. Thin Solid Films 2003;441:238–42.
[21] Fukumura T, Toyoaki H, Yamada Y. Semiconductors Science and Technology 2005;20:103–11.
[22] Batzill M, Katsiev Kh, Burst JM, Diebold U. Physical Review B 2005;72:165414.
[23] Weibel A, Bouchet R, Boulch F, Knauth P. Chemistry of Materials 2005;17:2378–85.
[24] Van der Pauw LJ. Philips Technical Review 1958/59;20(8):220–4.
[25] Banerjee AN, Chattopadhyay KK. Journal of Applied Physics 2005;97:084308.
[26] Bhat SV, Deepak FL. Solid State Communications 2005;135:345–7.
[27] Gopinadhan K, Pandya DK, Kashyap SC, Chaudhary S. Journal of Applied Physics 2006;99:126106.
[28] Fayat J, Castro MS. Journal of the European Ceramic Society 2003;23:1585–91.
[29] Lin Limei, Lai Fachun, Qu Yan, Gai Rongquan, Huang Zhigao. Materials Science and Engineering B 2007;138:166–71.
[30] Minami Tadatsugu. MRS Bulletin 2000.
[31] Lin Su-Shia, Huang Jow-Lay, Sajgalik P. Surface and Coatings Technology 2004;185:254–63.
[32] Feng YS, Yao RSh, Zhang LD. Chinese Physics Letters 2004;21:1374.